



# Butyrate rather than LPS subverts gingival epithelial homeostasis by downregulation of intercellular junctions and triggering pyroptosis

Juan Liu<sup>1</sup> | Yixiang Wang<sup>2</sup> | Huanxin Meng<sup>1</sup> | Jingting Yu<sup>3</sup> | Hongye Lu<sup>1</sup> |  
Wenjing Li<sup>1</sup> | Ruifang Lu<sup>1</sup> | Yibing Zhao<sup>1</sup> | Qiqiang Li<sup>4</sup> | Li Su<sup>5</sup>

<sup>1</sup>Department of Periodontology, Peking University School and Hospital of Stomatology, Beijing, China

<sup>2</sup>Central Laboratory, Department of Oral and Maxillofacial Surgery, Peking University School and Hospital of Stomatology, Beijing, China

<sup>3</sup>Department of General Dentistry II, Peking University School and Hospital of Stomatology, Beijing, China

<sup>4</sup>Department of Periodontology, Capital Medical University School of Stomatology, Beijing, China

<sup>5</sup>Center of Medical and Health Analysis, Peking University, Beijing, China

## Correspondence

Huanxin Meng, Department of Periodontology, Peking University School and Hospital of Stomatology, Zhongguancun Nandajie 22, Haidian District, Beijing 100081, China.

Email: kqhxmeng@bjmu.edu.cn

Yixiang Wang, Central Laboratory, Department of Oral and Maxillofacial Surgery, Peking University School and Hospital of Stomatology, Zhongguancun Nandajie 22, Haidian District, Beijing 100081, China.

Email: kqwangyx@bjmu.edu.cn

## Funding information

National Natural Science Foundation of China Science, Grant/Award Number: 81570980, 81772873 and 81870773

## Abstract

**Aim:** To investigate the effects of sodium butyrate (NaB) and lipopolysaccharide (LPS) on gingival epithelial barrier.

**Material and methods:** We cultured human primary gingival epithelial cells and investigated the effects of NaB and LPS on gingival epithelial barrier and involved mechanisms at in vitro and in vivo levels by immunostaining, confocal microscopy, field emission scanning electron microscopy (FE-SEM), transmission electronic microscopy (TEM), transepithelial electrical resistance (TEER), FTIC-dextran flux, flow cytometry, real-time PCR and Western blot assays.

**Results:** Our results showed that NaB, rather than LPS, destroyed the epithelial barrier by breaking down cell–cell junctions and triggering gingival epithelial cell pyroptosis with characteristic morphological changes, including swollen cells, large bubbles, pore formation in the plasma membrane and subcellular organelles changes. The upregulated expression of pyroptosis-related markers, caspase-3 and gasdermin-E (GSDME) contributed to this effect. Pyroptosis aroused by NaB is a pro-inflammatory cell death. Pyroptotic cell death provoked inflammatory responses by upregulation of IL-8 and MCP-1, and releasing intracellular contents into the extracellular microenvironment after pyroptotic rupture of the plasma membrane.

**Conclusions:** Our new findings indicate that butyrate is a potent destructive factor of gingival epithelial barrier and pro-inflammatory mediator, which shed a new light on our understanding of periodontitis initiation.

## KEYWORDS

butyrate, gingival epithelial barrier, inflammatory response, lipopolysaccharide, pyroptosis

## 1 | INTRODUCTION

Periodontal diseases place an enormous economic burden on the public health care system, and there was a 57.3% increase in the global burden from 1990 to 2010 (Jin et al., 2016; Tonetti, Jepsen, Jin, & Otomo-Corgel, 2017). The inflammatory status of periodontal diseases is highly related to the pathogenic gram-negative anaerobic

microorganisms, which carry many virulence factors including LPS, butyrate (bacterial metabolite) and so on (How, Song, & Chan, 2016; Yu et al., 2014). The key virulence factor, LPS, has been proven to be highly inflammatory to gingival fibroblasts or periodontal ligament cells, but not a potent inducer of inflammation in gingival epithelial cells (Darveau et al., 2004; Kusumoto et al., 2004). The gingival epithelia form the first line of periodontal defence and

play a critical role in protecting the underlying tissue against various harmful insults (Jin, 2011). The mucosa, which was considered merely a mechanical barrier, is now considered to be as a biological barrier too and plays a major role in the induction and maintenance of local immunity (Hammad & Lambrecht, 2015). Any breach of the barrier function results in the penetration of pathogens through the epithelium and arouses strong inflammatory reactions (Choi, Kim, Ji, & Choi, 2014; Groeger & Meyle, 2015; Meyle & Chapple, 2015). Because destruction of epithelium is the first step of periodontitis, the exploring of virulence factors responsible for penetrating the epithelial barrier and initiating the process of periodontitis is of great significance.

Butyrate is a metabolite of anaerobic bacteria. Tonetti and Singer raised a hypothesis that the short-chain fatty acids (including butyrate) were important virulence factors of anaerobic bacteria in periodontal diseases (Singer & Buckner, 1981; Tonetti et al., 1987). Inspired by these groundbreaking studies, we focused on this field and demonstrated that butyrate was highly related to the status of periodontal inflammation (Li, Meng, & Gao, 2012; Lu, Meng, Gao, Xu, & Feng, 2014). In addition, butyrate is demonstrated to inhibit the proliferation of gingival epithelial cells at low concentrations and to induce apoptotic or autophagic death at high concentrations (Evans et al., 2016; Tsuda, Ochiai, Suzuki, & Otsuka, 2010). Therefore, we supposed that butyrate might be an initiator of periodontitis and destroys the periodontal epithelial barrier.

Pyroptosis, a pro-inflammatory programmed necrosis, is characterized by cellular and nuclear swelling (Sun, Lu, Pervaiz, Cao, & Gan, 2005), balloon-shaped bubbles blowing around the nucleus (Fernandes-Alnemri et al., 2007), pores formation on plasma membrane (Chen et al., 2016; Liu et al., 2016; Russo et al., 2016) and release of pro-inflammatory mediators (LaRock & Cookson, 2013; Liu & Lieberman, 2017). Gasdermin-D (GSDMD) and gasdermin-E (GSDME) are two comparatively definite executioner of pyroptosis. GSDMD can be activated by caspase-1, caspase-4, caspase-5 and caspase-11 (Fink & Cookson, 2006; Kayagaki et al., 2015, 2013), while GSDME can only be activated by caspase-3 (Galluzzi & Kroemer, 2017; Rogers et al., 2017; Wang et al., 2017). Issues regarding whether and how butyrate destroys gingival epithelial barrier through pyroptosis and initiates inflammatory destruction of periodontitis remain largely unknown.

In this study, for the first time, we found that butyrate, rather than LPS, had the capability to destroy the epithelial barrier by triggering pyroptosis and downregulating the expression of intercellular junction proteins in human gingival epithelial cells (HGECs). Thus, our findings shed a new light on the initiation of periodontitis.

## 2 | MATERIALS AND METHODS

### 2.1 | Cell culture

Healthy human gingival tissues, following approval by the Ethics Committee of Peking University School and Hospital of Stomatology (PKUSSIRB-2011007), and with the written informed consent, were

### Clinical Relevance

*Scientific rationale for the study:* Butyrate and LPS are both closely associated with the inflammatory status of periodontitis. Which virulence factor conquers the first line of barrier and initiates the process of periodontitis, butyrate or LPS?

*Principal findings:* Butyrate rather than LPS subverted the gingival epithelial barrier function by triggering gingival epithelial cell pyroptosis and downregulating the expression of intercellular junction proteins.

*Practical implications:* The disturbing gingival epithelial homeostasis by butyrate opened a convenient door for the entry of periodontal pathogens and have a far-reaching effect on the initiation of periodontitis. The small molecular inhibitor, Z-VAD-fmk, may facilitate to prevent or treat periodontal disease.

obtained from healthy patients during third molar extraction procedures or crown lengthening surgery. Primary human gingival epithelial cells (HGECs) were cultured as described previously (Oda & Watson, 1990). Cultured HGECs were used between the second and fourth passages.

### 2.2 | Animal model

All animal care and experiments were performed in accordance with permission from the Laboratory of Animal Welfare Ethics of the Peking University Biomedical Ethics Committee (LA2018252). Sprague-Dawley (SD) rats (6–8 weeks old) were purchased from Vital River Laboratory Animal Technology and kept in a specific pathogen-free barrier facility with five animals in a cage. Fifteen rats were equally divided into three groups: placebo group (PBS), LPS group and NaB group. To mimic the in vivo status of LPS and butyrate, and to elucidate the influence of LPS and butyrate to gingival epithelium, LPS and NaB were applied to rats' gingival sulcus after anesthetizing with isoflurane. Considering the scouring effect of gingival crevicular fluid and saliva, we selected 50 mM NaB, five-fold doses of pathological state, as challenging dose. To coordinate with butyrate dose, 10 µg/ml LPS was selected. 4 µl PBS, LPS or NaB was injected into the palatal gingival crevice of the maxillary first and second molars of rats, at 5 min intervals for 5 times per day. The application was repeated every other day for 1 week. A section of tooth and periodontal tissue was preserved in 4% formalin for histopathological analysis.

### 2.3 | Transepithelial electrical resistance (TEER) and FITC-dextran transport assays

The permeability of the gingival epithelial barrier was measured by TEER. HGECs were seeded at a density of  $2.5 \times 10^5$  on a polyester

membrane transwell clear insert (diameter of 6.5 mm, pore size of 0.4  $\mu\text{m}$ , Corning 3,470; Corning Inc) and placed in 24-well culture plates (Corning). The TEER across the epithelium was measured with an EVOM (Epithelial Volt OhmMeter) with the subtraction of background resistance from cell-free inserts. HGECs were treated with 10 mM NaB or 1  $\mu\text{g}/\text{mL}$  LPS for 48 hr and TEER measurements were performed. The value was expressed as a percentage relative to the control group.

To further explore the permeability of the gingival epithelium, a FITC-dextran transport assay was applied. HGECs were seeded on polyester membrane inserts, as described above. HGECs were treated with 10 mM NaB or 1  $\mu\text{g}/\text{mL}$  LPS for 48 hr. FITC-dextran (molecular weight 70 kDa) was added to the upper chamber to give a concentration of 1 mg/ml and incubated for 30 min, and then 10  $\mu\text{l}$  medium from the lower chamber was collected to measure the fluorescence level using a multimode microplate reader at 520 nm

(EnSpire; PerkinElmer). Permeability of FITC-dextran was expressed as a percentage relative to the control group.

## 2.4 | Mitochondria morphological assays

To label mitochondria morphological changes, HGECs challenged with or without NaB were assessed by staining with Mito-Tracker green (Zhang et al., 2018).

Reagents, Biochemical assay, qRT-PCR, Western Blot Analysis, Histopathological Analysis, Immunocytochemistry Assay and Immunofluorescence, Field Emission Scanning Electron Microscopic (FE-SEM) and Transmission Electronic Microscopic (TEM) Observations and so on, See Appendix S1.

We selected 1, 5, 10 mM three concentrations for NaB which were within the scope of detection in periodontitis to test the morphological changes of gingival cells and cellular cytotoxicity, and all

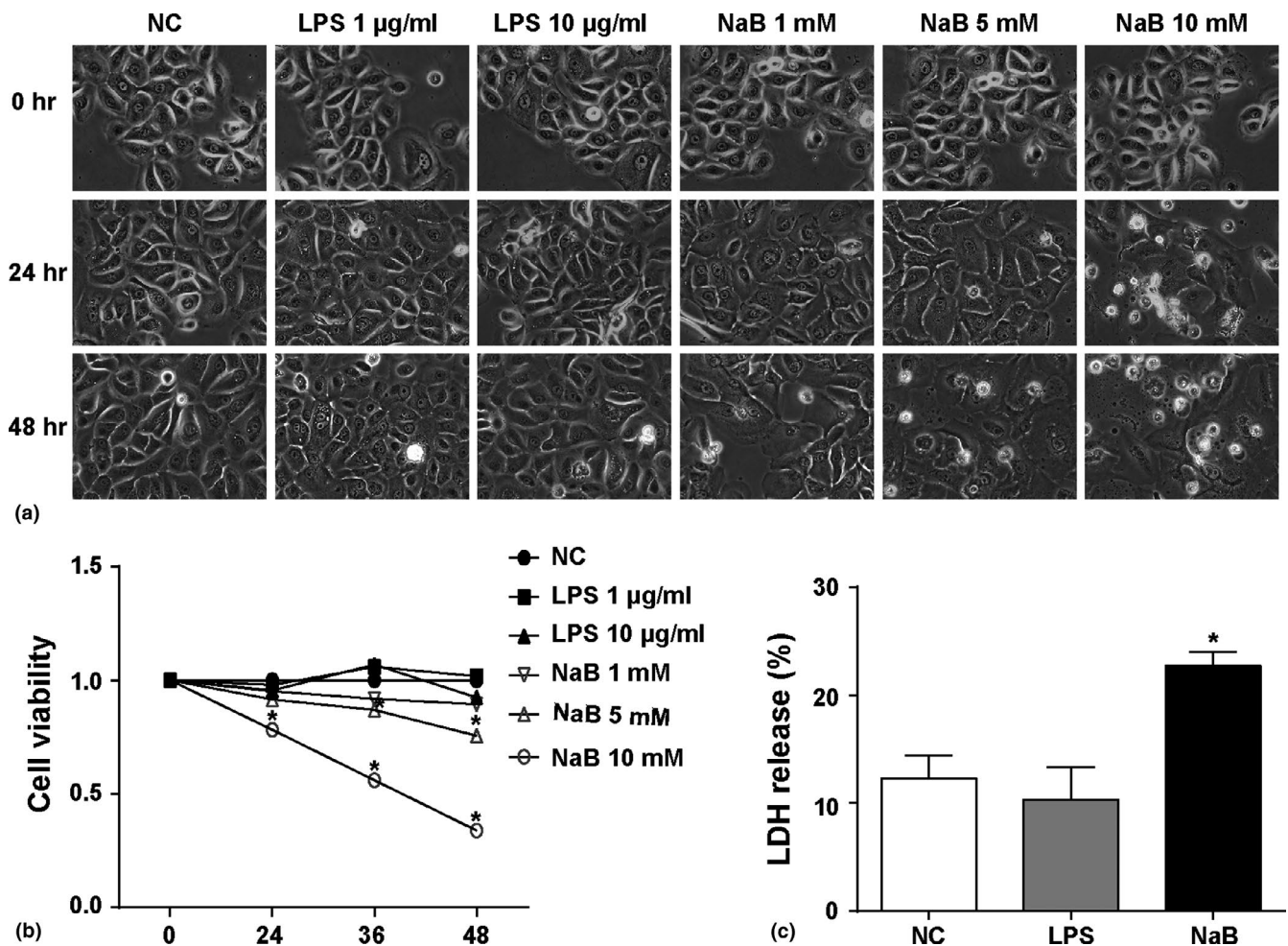


**FIGURE 1** NaB is a more potent virulence factor than LPS for HGECs. (a) Morphological observations of HGECs treated with LPS (1 or 10  $\mu\text{g}/\text{mL}$ ) or NaB (1, 5 or 10 mM) at 24 hr and 48 hr. (b) Cell viability analysis of HGECs treated with LPS (1 or 10  $\mu\text{g}/\text{mL}$ ) or NaB (1, 5 or 10 mM) at 24–48 hr ( $n = 3/\text{group}$ ; data are expressed as the means  $\pm$  SD;  $*p < 0.05$ , vs. NC,  $t$  test). (c) LDH release analysis of the plasma membrane damage of HGECs treated with 1  $\mu\text{g}/\text{mL}$  LPS or 10 mM NaB at 48 hr. LDH release (%) =  $100 \times (\text{experimental release} - \text{spontaneous release}) / (\text{maximum release} - \text{spontaneous release})$ . ( $n = 3/\text{group}$ ; data are expressed as the means  $\pm$  SD;  $*p < 0.05$ , vs. NC,  $t$  test). Abbreviation: NC, control

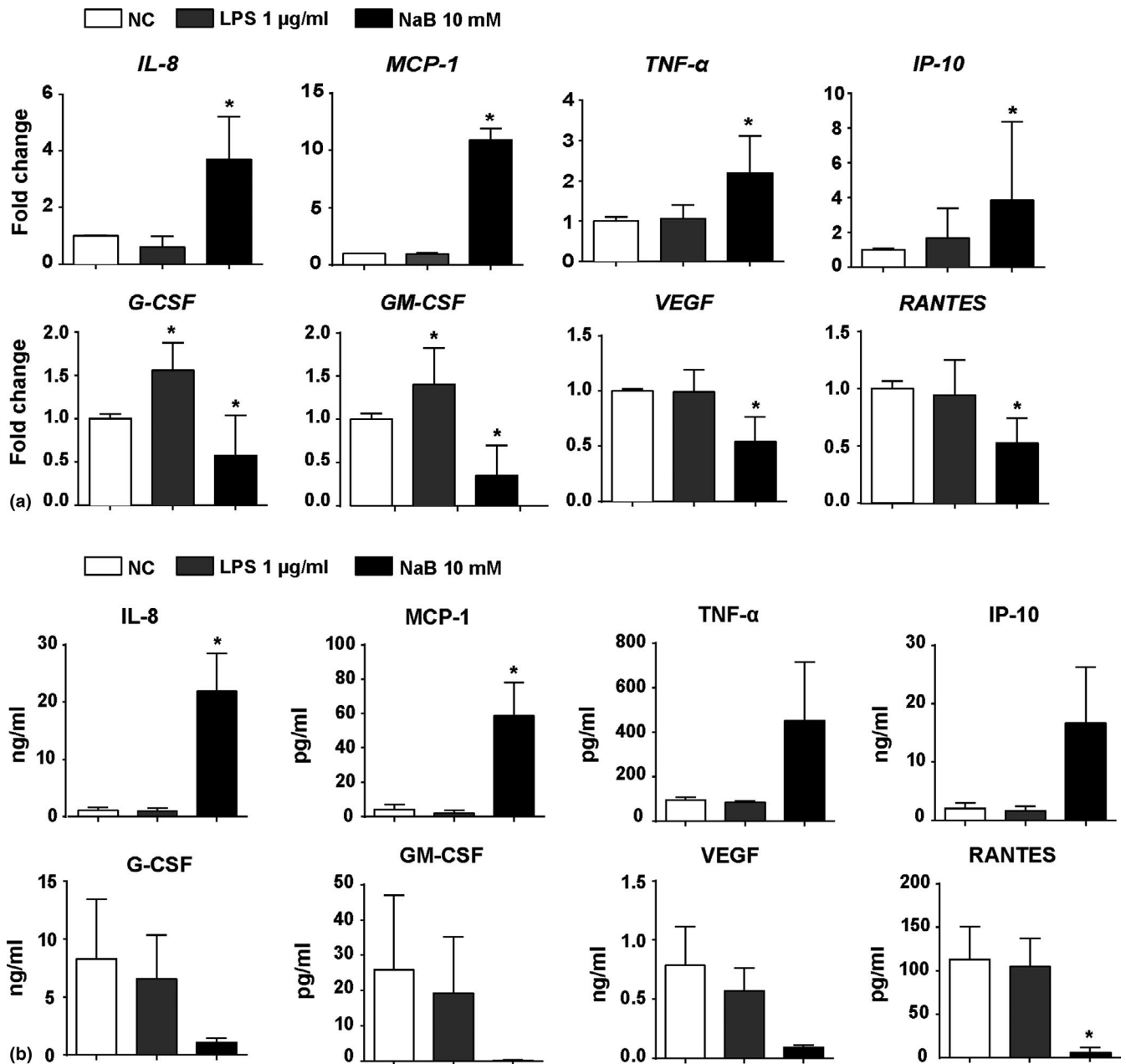


**FIGURE 2** NaB induces severer inflammatory response than LPS. (a) qRT-PCR analysis of *IL-8*, *MCP-1*, *TNF-α*, *IP-10*, *G-CSF*, *GM-CSF*, *VEGF* and *RANTES* mRNA level in HGECs challenged with 1 µg/mL LPS or 10 mM NaB at 24 hr ( $n = 3$ /group; data are expressed as the means  $\pm$  SD; \* $p < 0.05$ , vs. NC,  $t$  test). (b) Cell supernatant levels of *IL-8*, *MCP-1*, *TNF-α*, *IP-10*, *G-CSF*, *GM-CSF*, *VEGF* and *RANTES* were assayed in parallel at 48 hr after 1 µg/mL LPS or 10 mM NaB treatment ( $n = 3$ /group; data are expressed as the means  $\pm$  SD; \* $p < 0.05$ , vs. NC,  $t$  test). Abbreviation: NC, control. *IL-8*, interleukin-8. *MCP-1*, monocyte chemoattractant protein-1. *TNF-α*, tumour necrosis factor alpha. *IP-10*, interferon gamma-induced protein-10. *G-CSF*, granulocyte colony-stimulating factor. *GM-CSF*, granulocyte macrophage colony-stimulating factor. *VEGF*, vascular endothelial growth factor. *RANTES*, regulated upon activation normal T-cell expressed and secreted

the three concentrations of NaB showed cytotoxicity and cell morphological changes. In the subsequent experiments, 10 mM was used as the challenging dose. As for LPS, we chose 1 µg/ml and 10 µg/ml which far exceeds its pathological dose (36.8 pg/ml in the gingival crevicular fluid of rats in periodontitis) (Jiang et al., 2013). The two LPS doses had no cytotoxicity and did not change the morphology of HGECs, so we used 1 µg/ml LPS dose in the subsequent experiments except for the in vivo experiment.

### 3 | RESULTS

#### 3.1 | NaB is a more potent virulence factor than LPS for HGECs

To investigate the different effects of NaB and LPS, HGECs were treated with different concentration of LPS or NaB for the indicated times. Compared with the untreated control, LPS did not change cell morphology, which presented as cuboidal cells with



a big nucleocytoplasmic ratio exhibiting a paving stone shape (Figure 1a left). By contrast, when treated with NaB, HGECs became swollen and flat with blurred cellular contour (Figure 1a right). To quantify the cytotoxic effect of LPS and NaB, CCK-8 and lactate dehydrogenase (LDH) analyses were used. LPS had no cytotoxicity compared with the control, even at dosage of 10 µg/ml, while the cytotoxic effect of NaB occurred in a dose-dependent manner. NaB at a low concentration of 5 mM induced a significant increase in the number of dead cells. (Figure 1b) Meanwhile, LDH release assays showed that NaB induced more LDH release than LPS, which indicated that NaB had a stronger effect on cell membrane damage than LPS (Figure 1c). This indicates that NaB significantly affects the repair ability of periodontal tissue through a decrease in HGECs viability.

The interaction of bacterial virulence factors and host cells can modulate the expression profile of cytokines. We found that NaB upregulated the mRNA levels of interleukin-8 (IL-8), monocyte chemoattractant protein-1 (MCP-1), tumour necrosis factor-α (TNF-α), interferon-inducible protein-10 (IP-10) and downregulated the expression of granulocyte colony-stimulating factor (G-CSF), granulocyte macrophage colony-stimulating factor (GM-CSF), vascular endothelial growth factor (VEGF) and regulated on activation, normally T cell expressed and secreted (RANTES) (Figure 2a). The virulence factor, LPS, had no influence in the expression of the majority of above cytokines, except for G-CSF and GM-CSF (Figure 2a). Cytokine array assays confirmed the qRT-PCR results at the protein level by detecting culture supernatants derived from HGECs challenged with LPS or NaB. NaB significantly altered the expression profiles of the above cytokines in HGECs, while LPS did not change their expression. Importantly, two key inflammatory chemokines in periodontitis, IL-8 and MCP-1, were markedly increased at both the mRNA and protein levels in NaB-treated HGECs compared with control and LPS groups (Figure 2a). The results suggest that NaB is a more potent virulence factor than LPS in gingival epithelial cells in periodontitis.

### 3.2 | NaB, rather than LPS, disturbs gingival epithelial homeostasis

Gingival epithelia form the first line of innate defence (gingival epithelial barrier) against various irritations from microorganisms and physicochemical factors. To compare the effects of NaB and LPS on the gingival epithelial barrier, the *in vitro* gingival epithelial barrier, a multilayer of HGECs (3-dimensional epithelial culture) model, and animal experiments were used. NaB or LPS was applied to the multilayer epithelium for 48 hr, and then, the integrity of the gingival epithelial barrier was evaluated by TEER, epithelial permeability analysis and confocal microscopy. TEER results showed that the electricity resistance value was markedly decreased only in NaB-treated group (Figure 3a left). To further verify the epithelial barrier destruction effect of NaB, an epithelial permeability assay was applied using the detection of 70 kDa FITC-dextran. The results showed that NaB increased FITC-dextran flux through

gingival epithelial layer, which was in line with TEER results (Figure 3a right). TEM images showed that HGECs were packed tightly with 5–6 layers in the control or LPS treated groups. Fewer layers of sparsely distributed epithelial cells with disturbed intercellular junctions were found in NaB-treated group (Figure 3b). Three-dimensionally reconstructed micrographs of multilayer epithelial mimics further clarified the epithelial destruction function of NaB, with reduced thickness and sparse intercellular gaps (Figure 3c).

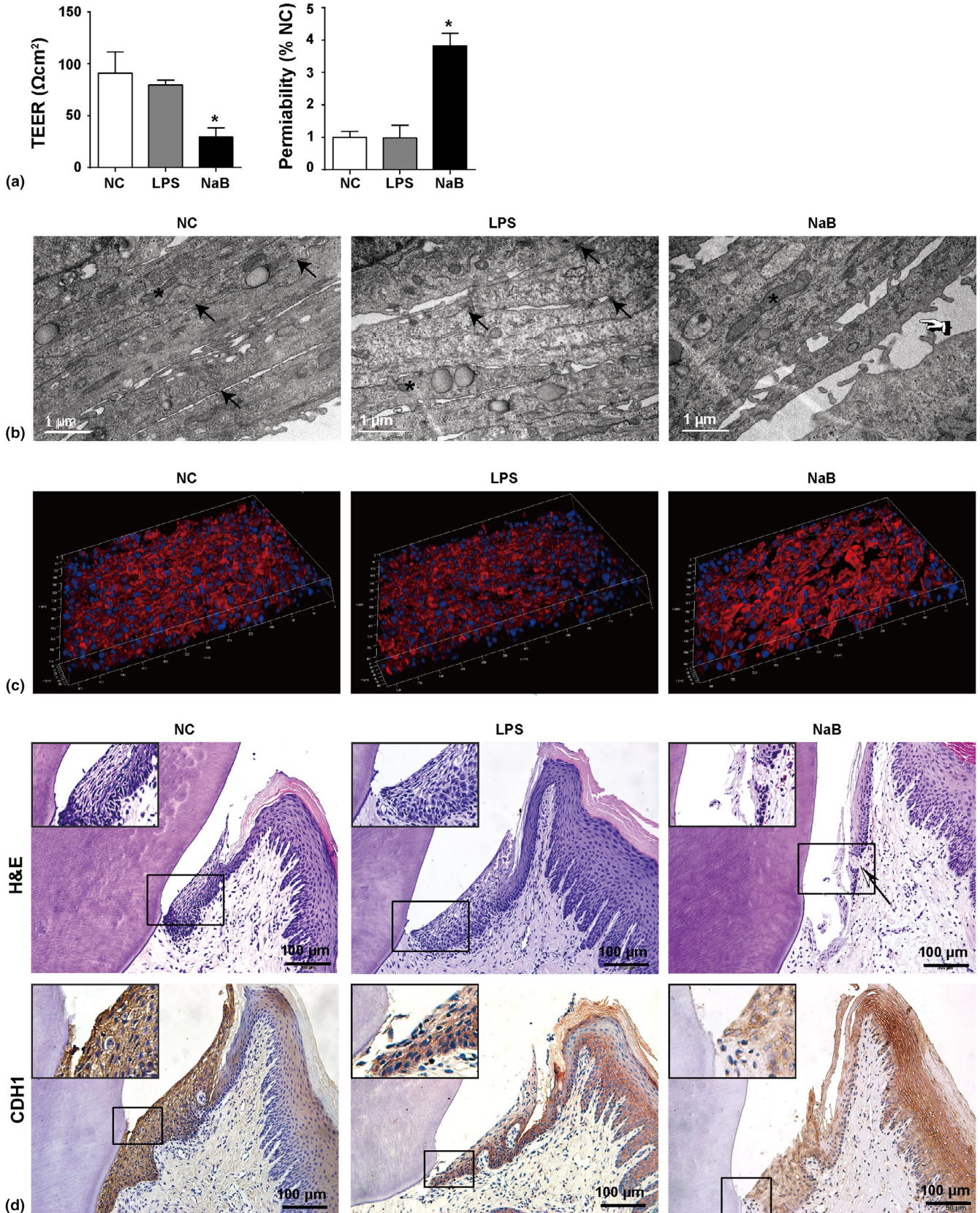
The *in vivo* experiments corroborated epithelial barrier disturbing effects of NaB. After treatment with NaB, the number of epithelial layers of junctional epithelium decreased, and cells became loose with large intercellular spaces. Meanwhile, angiogenesis in subepithelial connective tissue was obvious (Figure 3d up panel). The gingival epithelial cells from NaB-treated rats showed swollen and weaker staining with CDH1 (E-cadherin) compared with control group or LPS group (Figure 3d down panel).

Cell junctions build up the barrier of epithelia by connecting neighbouring cells. Adherent junctions and tight junctions are essential for the gingival epithelial barrier function. To investigate the effects of NaB or LPS on the expression of intercellular junction markers *in vitro*, the mRNA levels of gap junction genes *CX26* (connexin 26) and *CX43* (connexin 43), adherence junction gene *CDH1*, tight junction genes *JAM-1* (junctional adhesion molecule-1), *CLDN1* (claudin-1) and *CLDN4* (claudin-4), desmosome genes *DSG1* (desmoglein-1) and *DSC2* (desmocollin-2) were analysed by qRT-PCR. The results showed that LPS did not affect the expression of these genes, while NaB significantly downregulated their expression (Figure 4a). Meanwhile, immunostaining showed that the adherence junction protein, E-cadherin, and tight junction protein, claudin-1, were severely disturbed by NaB, rather than LPS (Figure 4b), which indicates that NaB, rather than LPS, disturbs the gingival epithelial barrier.

### 3.3 | NaB triggered pyroptotic cell death of HGECs

To determine the type of cell death caused by NaB, NaB-induced cell morphological changes were monitored with an IncuCyte Zoom<sup>TM</sup> live cell imaging system (Essen BioScience) and phase microscopy. The results showed that HGECs became swollen with reduced cell membrane refraction at 24 hr after NaB treatment, and cells were swollen further with fuzzy cell boundaries at 48 hr after NaB treatment (Figure 1a). In addition, some of cells died and displayed large bubbles (Figure 5a). The results were further confirmed by haematoxylin & eosin (H&E) staining of NaB-treated cells (Figure 5b). Additionally, HGECs treated with NaB were approximately four times the size of HGECs in the control group. The nucleocytoplasmic ratio was reduced and cells exhibited a flattened pattern with fine, long protuberances trying to contact neighbouring cells.

Under SEM and TEM examination, we found that, in addition to swollen cells with large bubbles, another morphological characteristic was the formation of pores in the cellular membrane. Pore size ranged from 200 nm to 800 nm. Additionally, the number of



microvilli on the membrane surface was decreased in NaB-treated cells compared to untreated control cells (Figure 5c). NaB can cause pyroptosis. We next aimed to understand what is happening at

subcellular structural level after NaB treatment. TEM showed that mitochondria were swollen in NaB-challenged HGECs (Figure 5d). The mitochondria were further addressed using Mito-Tracker dyes



**FIGURE 3** Effects of NaB and LPS on gingival epithelial barrier. (a) TEER of multilayer HGECs stimulated by 1  $\mu\text{g}/\text{ml}$  LPS or 10 mM NaB for 48 hr; gingival epithelial permeability analysis of multilayer HGECs stimulated by 1  $\mu\text{g}/\text{ml}$  LPS or 10 mM NaB for 48 hr ( $n = 3/\text{group}$ ; data are expressed as the means  $\pm$  SD; \*  $p < 0.05$ , vs. NC,  $t$  test). (b) TEM images of cell layers of HGECs and intercellular junctions after treatment with 1  $\mu\text{g}/\text{ml}$  LPS or 10 mM NaB for 48 hr.  $\kappa$ , intercellular junction;  $\rho$ , intercellular gap; \*, mitochondria. (c) Representative photomicrographs of immunofluorescence staining for pan-keratin (red) of multilayer HGECs cultured on collagen treated with 1  $\mu\text{g}/\text{ml}$  LPS or 10 mM NaB for 48 hr. The nuclei (blue) were counterstained with DAPI. (d) Representative images of H&E-stained and CDH1 stained gingival tissue treated with PBS, 10  $\mu\text{g}/\text{ml}$  LPS or 50 mM NaB. High-power fields with magnified details were displayed in the upper left corner of the original images.  $\kappa$ , junctional epithelium destruction. Abbreviation: NC, control. CDH1, E-cadherin

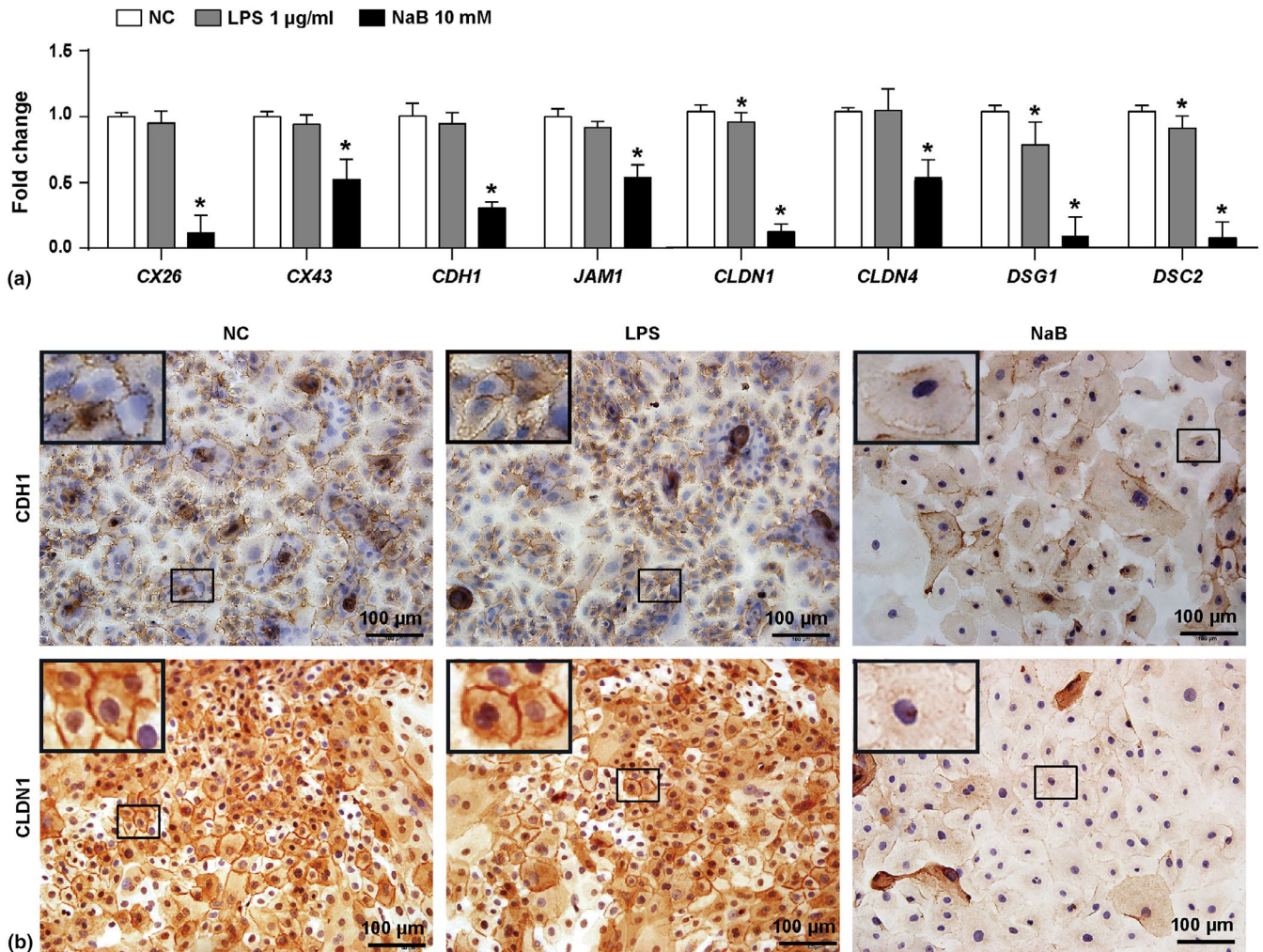


**FIGURE 4** Effects of NaB and LPS on expression of intercellular junction-related genes of HGECs. (a) qRT-PCR analysis of mRNA levels of the intercellular junction-related genes, *CX26*, *CX43*, *CDH1*, *JAM1*, *CLDN1*, *CLDN4*, *DSG1* and *DSC2* in HGECs challenged with 1  $\mu\text{g}/\text{ml}$  LPS or 10 mM NaB at 24 hr ( $n = 3/\text{group}$ ; data are expressed as the means  $\pm$  SD; \*  $p < 0.05$ , vs. NC,  $t$  test). (b) Representative images of CDH1 and CLDN1 immunostaining in untreated (NC), 1  $\mu\text{g}/\text{ml}$  LPS or 10 mM NaB-treated HGECs groups. Abbreviation: NC, control. *CX26*, connexin 26. *CX43*, connexin 43. *CDH1*, E-cadherin. *JAM1*, junctional adhesion molecule-1. *CLDN1*, claudin-1. *CLDN4*, claudin-4. *DSG1*, desmoglein-1. *DSC2*, desmocollin-2

during NaB treatment. The results showed that the mitochondria lost their normal morphologies and became swollen and fragmented (Figure 5e). The functional consequences of NaB-related morphological changes in the mitochondria included a decrease in mitochondrial membrane potential and impaired ATP production (Figure 5e). The above results indicated that NaB perhaps causes dysfunctions in the mitochondria, which triggered cascade responses that ultimately lead to cell pyroptosis.

### 3.4 | NaB induced pyroptosis through caspases cascade-mediated GSDME activation

Of the key pyroptosis-associated proteins, caspases are highly expressed in the mitochondria and gasdermins are mainly expressed in epithelial tissues. Based on this, we focused on these two families to explore the mechanism of pyroptosis in HGECs after NaB treatment. Confocal microscopy and flow cytometry showed that caspases

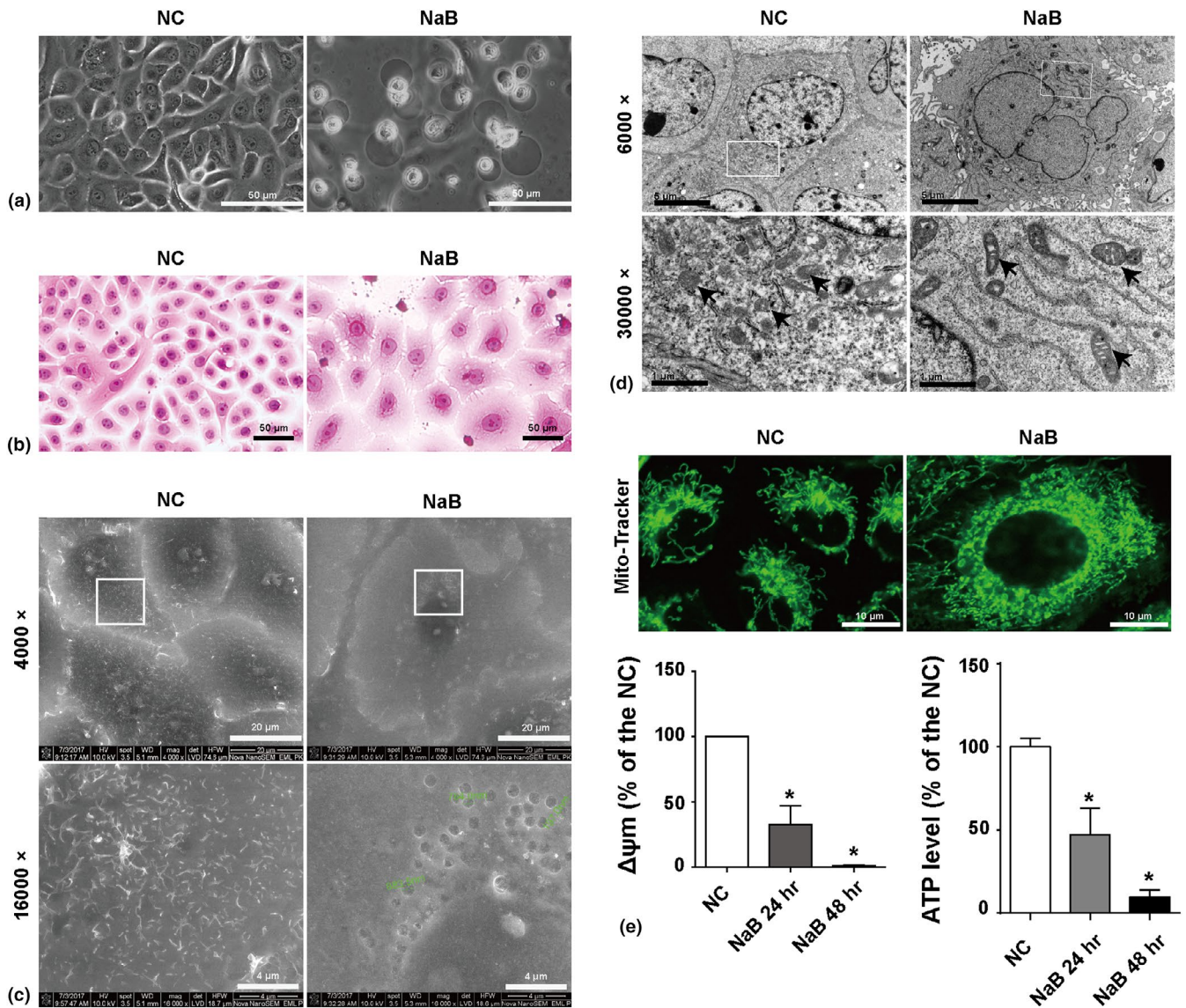


**FIGURE 5** NaB induced pyroptotic cell death. HGECs were treated with 10 mM NaB for 48 hr. (a) Representative phase-contrast images of pyroptotic cells (with large bubbles extending from the plasma membrane). (b) Representative H&E-stained images of pyroptotic cells (swollen cells). (c) Representative SEM images of pyroptotic cells (multiple cell membrane pores). (d) Representative TEM images of pyroptotic cells.  $\blacktriangledown$ , mitochondrion. (e) Representative confocal images of mitochondria, cellular ATP levels ( $n = 3$ ) and mitochondrial membrane potentials ( $n = 2$ ) in HGECs at basal conditions and after exposure to 10 mM NaB for 24 hr and 48 hr (data are expressed as the means  $\pm$  SD; \*  $p < 0.05$ , vs. NC,  $t$  test). Abbreviation: NC, control

were activated in NaB-treated HGECs (Figure 6a). The expression of the caspase family was assessed by qRT-PCR, and caspase-9 was the most highly expressed member of the caspase family (Figure 6b). The canonical and non-canonical pyroptotic pathway markers, caspase-1, caspase-5 and GSDMD were examined by Western blot. GSDMD, the executor of canonical and non-canonical pyroptotic pathway, was not upregulated or activated by NaB. NaB slightly increased the expression of caspase-1 and caspase-5 at the 12 h and 24 h time points (Figure 7a). Inflammatory factors IL-1 $\beta$  and IL-18 were undetectable by using ELISA kits (data not shown). The active forms of caspase-9, caspase-3 and GSDME were upregulated in NaB-treated cells (Figure 7b). To prove that the N-terminus of GSDME (GSDME-N) rather than GSDMD-N has the ability to form pores in

the plasma membrane, we extracted the membrane proteins and found that GSDME-N was enriched in NaB-treated cells compared to the control group, while with regard to GSDMD-N, no difference was observed between control cells and NaB-treated cells (7c). With the pretreatment of HGECs with Z-VAD-FMK (a pan-caspase inhibitor), the expression levels of the cleaved forms of GSDME decreased (7d), and the number of dead cells decreased significantly (Figure S3).

## 4 | DISCUSSIONS

The gingival epithelium, which has both physical and biological barrier functions, is the first line of defence against bacteria and their



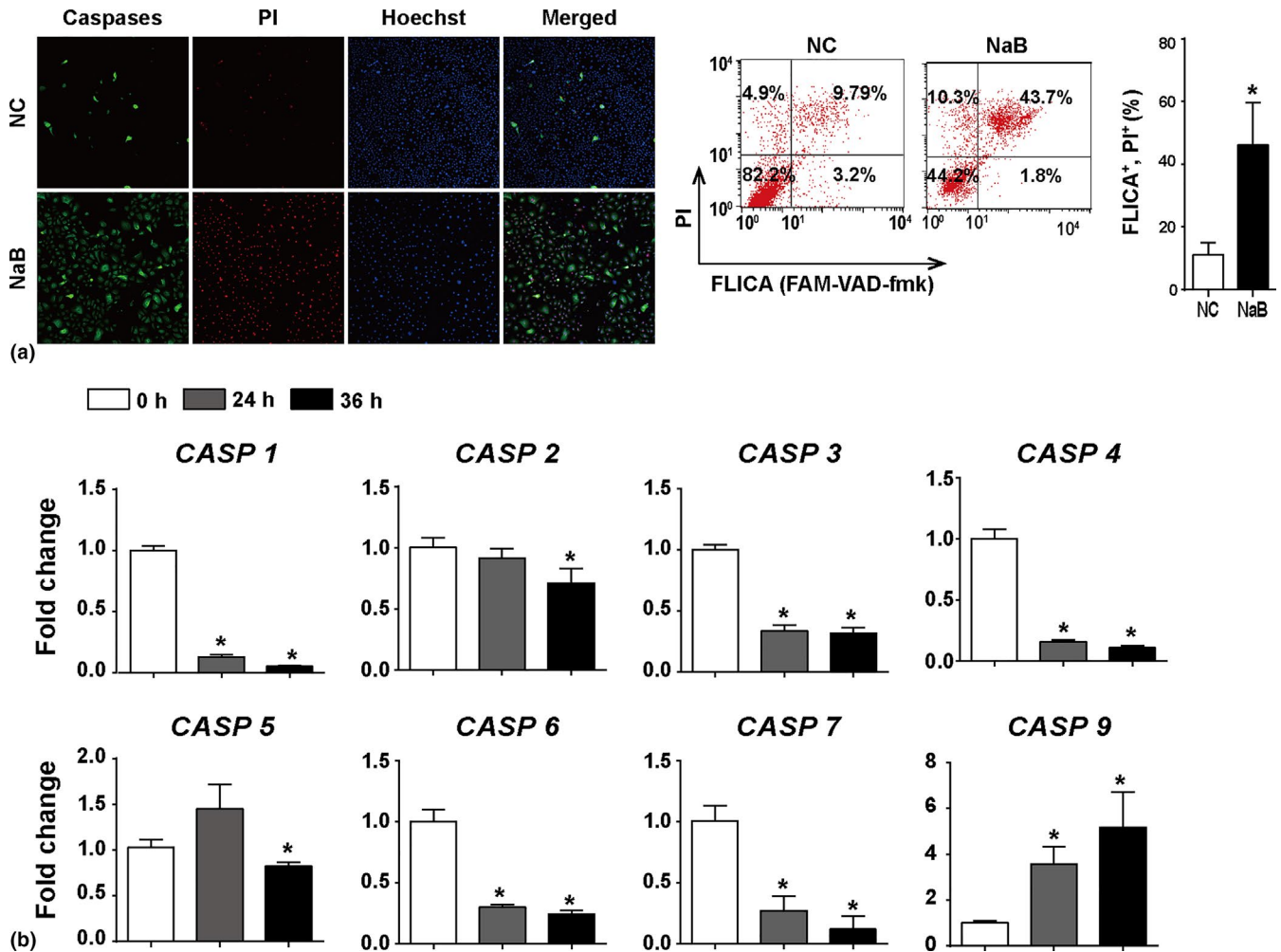


**FIGURE 6** Caspases family is activated by NaB. (a) Representative confocal images and flow cytometry of HGECs treated with 10 mM NaB for 48 hr. Activated caspases were revealed by FAM-VAD-fmk FLICA (green channel), PI-labelled nuclei of dead cells (red channel) and Hoechst stained nuclei of live cells (blue channel). The FLICA and PI double positive cells were analysed ( $n = 3$ ; data are expressed as the means  $\pm$  SD; \*  $p < 0.05$ , vs. NC,  $t$  test). (b) qRT-PCR analysis of the mRNA level of caspases in HGECs challenged with 10 mM NaB for the indicated time ( $n = 3$ ; data are expressed as the means  $\pm$  SD; \*  $p < 0.05$ , vs. NC,  $t$  test). Abbreviation: NC, control

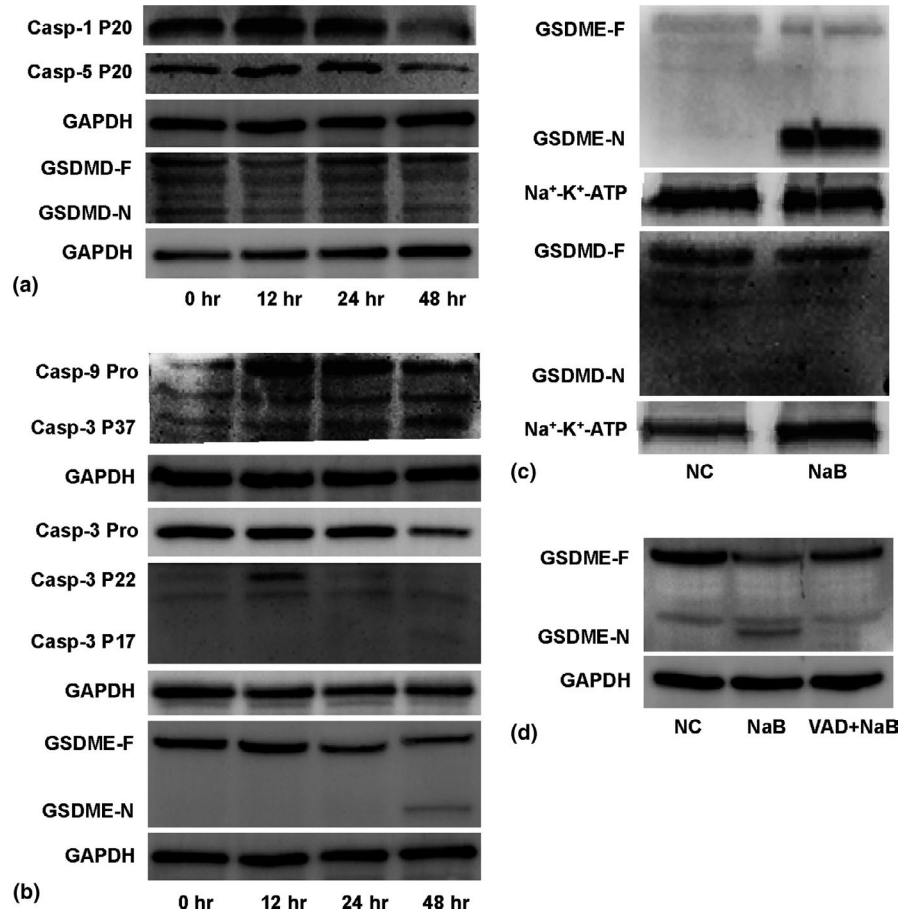
virulent challenge (Groeger & Meyle, 2015). A breakdown of the gingival epithelial barrier initiates periodontal diseases (Choi et al., 2014). Identifying the main contributor to the destruction of the gingival epithelial barrier would be greatly beneficial in preventing and solving periodontal issues.

By comparing NaB with LPS in gingival epithelial barrier function, we verify for the first time that butyrate is a potent destructor of the gingival epithelial barrier. The concept that butyrate's contributing to periodontal inflammation is initially postulated by Singer and is re-affirmed by Tonetti (Singer & Buckner, 1981; Tonetti et al., 1987). Our clinical data clearly show that butyrate is present at a high level in patients with periodontitis and is closely associated with the periodontal inflammatory status (Li et al., 2012; Lu et al., 2014). This result is in line with previous studies (Niderman, Buyle-Bodin, Lu, Robinson, & Naleway, 1997a; Niderman, Zhang, & Kashket, 1997b). Interestingly, previous studies show that NaB has the ability to inhibit gingival epithelial cell growth and induce apoptosis of gingival epithelial cells (Ebe et al., 2011; Evans et al., 2016; Tsuda et al., 2010).

This means that NaB probably acts as a gingival epithelial barrier destructor during the process of periodontitis. To verify this hypothesis, we compared the effects of the two important bacterial virulence factors, NaB and LPS, on the destruction of the gingival epithelial barrier by using primary HGECs, 3D epithelial cell cultures and an animal challenge model. Our results clearly show that NaB plays a role in the destruction of the gingival epithelial barrier by reducing the expressive level of intercellular junctions and inducing cell death, whereas LPS has no obviously destructive effects on gingival epithelial cells. The evidences overall illustrate that butyrate, rather than LPS, acts as a potent gingival epithelial barrier destructor and plays an important role in initiating periodontitis.

Importantly, butyrate kills gingival epithelial cells in more than one way. Previous *in vitro* studies have shown that butyrate induces apoptosis, autophagy and necrosis-dependent cell death of gingival epithelial cells (Astakhova et al., 2016; Ebe et al., 2011; Tsuda et al., 2010). In this study, we identify a new programmed cell death caused by butyrate, pyroptosis, which displayed typical morphological

**FIGURE 7** The mechanism of pyroptosis induced by NaB. (a) Western blot analysis of canonical and non-canonical pyroptotic death-related protein (caspase-1, caspase-5, and GSDMD) expression in HGECS from the control group or the 10 mM NaB-treated group at the indicated time points. (b) Western blot analysis of the full length and active forms of caspase-9, caspase-3, GSDME protein expression in HGECS from the control group or the 10 mM NaB-treated group at the indicated times. (c) Western blot analysis of GSDMD-N and GSDME-N expression in the plasma membrane after 10 mM NaB exposure for 48 hr. (d) Western blot analysis of GSDME protein expression in HGECS exposed to 10 mM NaB for 48 hr with or without 50  $\mu$ M Z-VAD-fmk (VAD) pretreatment for 1 hr. Abbreviation: NC, control



(swollen cells and organelles, plasma membrane pores, large bubbles) and molecular changes (activated caspase cascade proteins, activated GSDME) (Chen et al., 2016; Ebe et al., 2011; Fernandes-Alnemri et al., 2007; Liu et al., 2016; Russo et al., 2016; Sun et al., 2005). Pyroptosis has been classified as caspase-1 dependent canonical and caspase-11 (human caspase-4 or caspase-5) dependent non-canonical inflammasome signal pathways, which were orchestrated by GSDMD (Broz, 2015). Recent studies have shed a light on the mechanisms of caspase-3/GSDME-induced secondary necrosis/pyroptosis (Broz, 2015; Rogers et al., 2017). GSDME is cleaved by activated caspase-3, and the GSDME-N assembles within the plasma membrane to form pores and permeabilize the plasma membrane (Broz, 2015; Rogers et al., 2017). In our study, caspase-1 and caspase-5 were slightly activated by NaB, but the expressive level of GSDMD-N showed no difference between control group and NaB-treated group. It demonstrated that GSDMD was not involved in the pyroptosis triggered by NaB. In this study, the GSDME was highly expressed by HGECS and activated by NaB. The same results were confirmed by using high concentration of NaB (50 mM) (Figures S1–S3). Based on the above evidences, we deduced that butyrate induces pyroptosis probably through a caspase-3/GSDME axis, but not through the canonical caspase-1-dependent or the non-canonical caspase-4/-5-mediated inflammasome signalling pathways. To date, the underlying mechanisms regarding how NaB induces cell death remain largely unknown and further investigation is needed.

Mitochondria are energy-producing organelles, which exist in most cells. Mitochondria play a critical role during apoptosis and pyroptosis. The morphological changes of mitochondria, such as swelling or flocculent density, are considered as signs of necrosis (Kerr, Gobe, Winterford, & Harmon, 1995). Mitochondria decay precedes pyroptotic plasma membrane rupture (de Vasconcelos, Opdenbosch, Gorp, Parthoens, & Lamkanfi, 2018). With the increase of mitochondria permeability, the progression of cell death becomes irreversible (Nakagawa et al., 2005). Morphological and dysfunctional changes of mitochondria were observed in pyroptotic epithelial cells in this study. Mitochondria got swollen and fragmented. Functional consequences of NaB-related morphological changes of mitochondria were a decrease of mitochondria membrane potential and impaired ATP production. Studies have shown that dysfunctional mitochondria release excessive ROS, which can activate inflammasomes and promote the occurrence of pyroptosis (Lian et al., 2018; Zhou, Yazdi, Menu, & Tschopp, 2011). Mitochondria damage is upstream or downstream of the NLRP3 and AIM2 inflammasomes (Allam et al., 2014; Zhou et al., 2011). The intrinsic apoptotic pathway leads to robust activation of caspase-9, the cleaved caspase-9 can activate apoptotic caspase-7 and pyroptotic caspase-3 (Zhang et al., 2019).

Pyroptotic cell death induced by butyrate provokes inflammatory responses. Just as the term “pyroptosis” implies, “pyro” means fever and “ptosis” implies falling (Bergsbaken, Fink, & Cookson, 2009; Vande Walle & Lamkanfi, 2016). In the canonical inflammasome



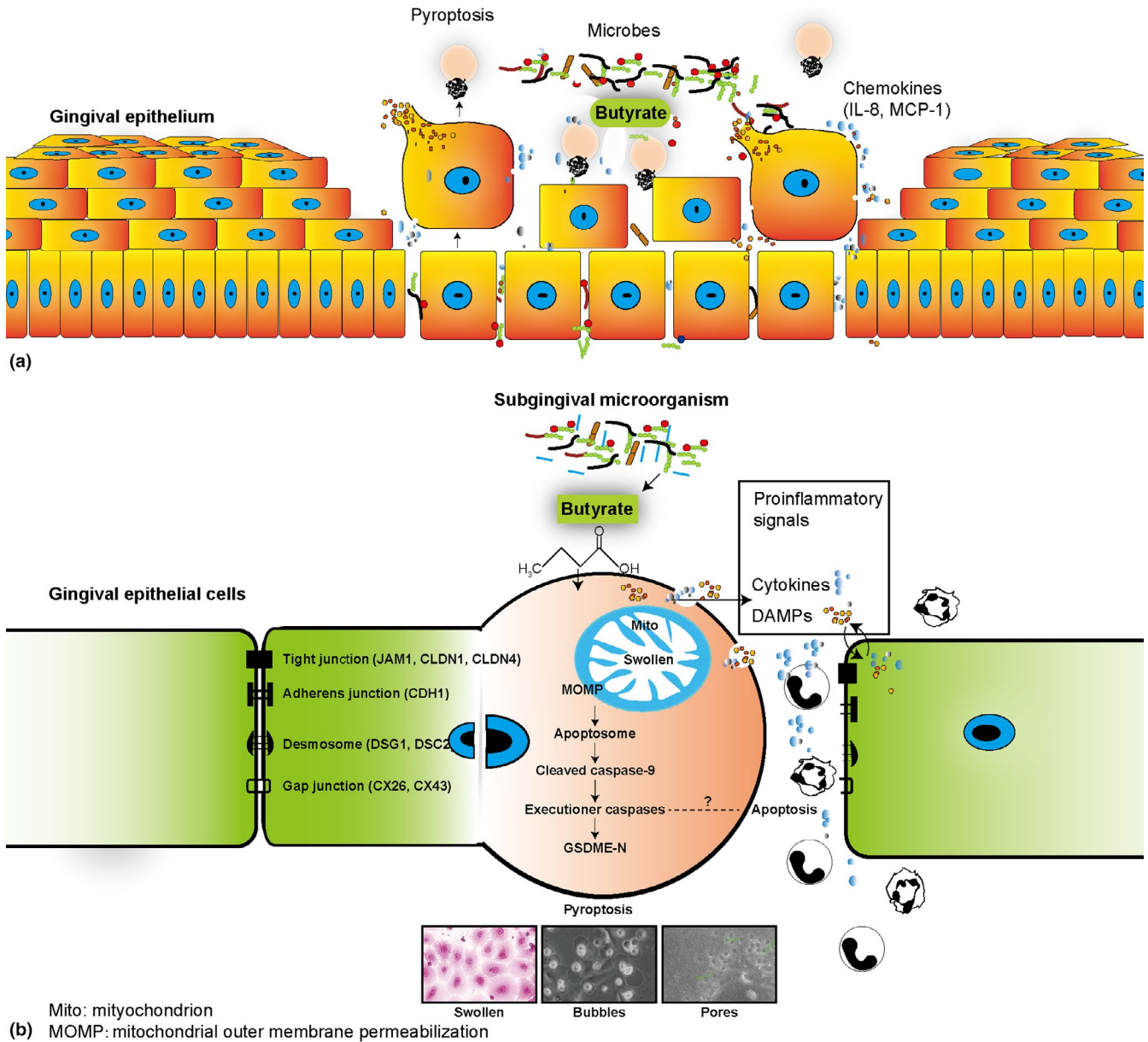


**FIGURE 8** Schema of butyrate disturbing gingival epithelial homeostasis. (a) Butyrate, a bacteria metabolite, destroys the integrity of gingival epithelium by triggering pyroptosis of gingival epithelial cells, destroying intercellular junctions and inducing gingival epithelial cells to secrete chemokines, IL-8 and MCP-1. (b) The mitochondria become swollen and the mitochondrial outer membrane permeabilization increases after the cells treated with butyrate. Meanwhile, caspase-9 is activated and triggers caspase-3/GSDME-dependent pyroptosis. GSDME-N enriches in the cytoplasmic membrane and forms pores in the cellular membrane, finally leading to cell swollen and bubble. The pro-inflammatory signals, such as chemokines (IL-8 and MCP-1) and damage-associated molecular patterns (DAMPs) are released to induce inflammatory response. With the occurrence of pyroptosis, the structure of gingival epithelial junctions (tight junction, adherent junction, desmosome and gap junction) are destroyed through downregulation of intercellular junction-associated genes including CX26, CX43, CDH1, JAM1, CLDN1, CLDN4, DSG1 and DSC2. Abbreviation: NC, control. CX26, connexin 26. CX43, connexin 43. CDH1, E-cadherin. JAM1, junctional adhesion molecule-1. CLDN1, claudin-1. CLDN4, claudin-4. DSG1, desmoglein-1. DSC2, desmocollin-2

pathway, the inflammatory cytokines pro-IL-1 $\beta$  and pro-IL-18 are processed into their mature forms by caspase-1, and then the mature cytokines may be released as secondary events of pyroptotic cell lysis or may be actively secreted independent of cell lysis (Chen et al., 2014; He et al., 2015; Russo et al., 2016). In addition, pyroptotic rupture of the plasma membrane poses the threat of intracellular contents being released into the extracellular microenvironment (LaRock & Cookson,

2013; Lu, Wang, Andersson, & Tracey, 2013). These endogenous components, including high-mobility group box 1, ATP, S100 protein, heat shock protein and IL-1 family proteins, served as alarmins and damage-associated molecular patterns, are highly pro-inflammatory in the extracellular milieu and are involved in innate immunity and inflammatory responses through the activation of pattern recognition receptors on host cells (Brydges et al., 2013; Chen & Nunez,

2010). According to previous studies, elevated level of extracellular high-mobility group box 1, ATP, S100 protein and heat shock protein becomes the focus of attention in periodontitis (Binderman, Gadban, & Yaffe, 2017; Nethravathy, Alamelu, Arun, & Kumar, 2014; Sun et al., 2011; Tsybikov, Baranov, Kuznik, Malezhik, & Isakova, 2014; Xie, Deng, Gong, Ding, & Tang, 2011). Caspase-3 rather than caspase-1 is activated in the pyroptotic cell death aroused by butyrate, so IL-1 $\beta$  and IL-18 are not upregulated. High-mobility group box 1 is released by damaged gingival epithelial cells when challenged by butyrate (Ebe et al., 2011). Additionally, the pyroptotic HGECs challenged with butyrate robustly released the inflammatory cytokines, IL-8 and MCP-1, which are closely related to periodontitis. (Thunell et al., 2010) Polymorphonuclear neutrophils, which, attracted by the gradient of IL-8 secreted from HGECs in response to pathogenic stimuli, dominate the early response phase of periodontitis (Kusumoto et al., 2004). Polymorphonuclear neutrophils relieve the inflammatory status by enhancing phagocytic activity or elicit a sustained chronic inflammatory status by secreting inflammatory mediators (Herrmann & Meyle, 2015). Monocytes, which also participate in the battle between the host and microbes at the very early stages of infection, are mobilized following a gradient of MCP-1 (Smith, Seymour, & Cullinan, 2010). The pyroptotic cell death aroused by butyrate may initiate periodontitis by releasing damage-associated molecular patterns or the chemokines, IL-8 and MCP-1.

We cannot deny the pro-inflammatory effects of LPS to mesenchymal cells such as gingival fibroblasts or periodontal ligament cells, but LPS is not a potent inducer of inflammation of gingival epithelial cells (Darveau et al., 2004; Kusumoto et al., 2004).

In summary, our new findings show that butyrate, rather than LPS, destroys the periodontal epithelial barrier by downregulation the expression of cell-cell junctions and activating the caspase-3/GSDME-mediated epithelial pyroptotic cell death of HGECs (Figure 8). Butyrate, rather than LPS, is a potent gingival epithelial barrier destructive factor, and these data shed new light on the elucidation of the initiation of periodontitis.

## ACKNOWLEDGEMENTS

This study was supported by grants from National Natural Science Foundation of China Science (81570980, 81772873 and 81870773). The authors declare no potential conflicts of interest with respect to the authorship and/or publication of this article. We thank professors Feng Shao and Liling Wu for technical assistance, Li Xu, Wei Qi and Yanrui Feng for helping collecting gingival tissues. We would like to thank the State Key Laboratory of Membrane Biology, Institute of Zoology, Chinese Academy of Sciences and we would be grateful to Yinzi Ma and Pengyan Xia for their help of making TEM sample and cutting ultrathin section.

## CONFLICT OF INTEREST

The authors have stated explicitly that there are no conflicts of interest in connection with this article.

## ORCID

Juan Liu  <https://orcid.org/0000-0002-5403-1473>

Huanxin Meng  <https://orcid.org/0000-0002-2954-818X>

Wenjing Li  <https://orcid.org/0000-0002-9905-3836>

## REFERENCES

- Allam, R., Lawlor, K. E., Yu, E. C., Mildenhall, A. L., Moujalled, D. M., Lewis, R. S., ... Vince, J. E. (2014). Mitochondrial apoptosis is dispensable for NLRP3 inflammasome activation but non-apoptotic caspase-8 is required for inflammasome priming. *EMBO Reports*, 15, 982–990. <https://doi.org/10.15252/embr.201438463>
- Astakhova, L., Ngara, M., Babich, O., Prosekov, A., Asyakina, L., Dyshlyuk, L., ... Matskova, L. (2016). Short chain fatty acids (SCFA) reprogram gene expression in human malignant epithelial and lymphoid cells. *PLoS ONE*, 11, 1–18. <https://doi.org/10.1371/journal.pone.0154102>
- Bergsbaken, T., Fink, S. L., & Cookson, B. T. (2009). Pyroptosis: Host cell death and inflammation. *Nature Reviews Microbiology*, 7, 99–109. <https://doi.org/10.1038/nrmicro2070>
- Binderman, I., Gadban, N., & Yaffe, A. (2017). Extracellular ATP is a key modulator of alveolar bone loss in periodontitis. *Archives of Oral Biology*, 81, 131–135. <https://doi.org/10.1016/j.archoralbio.2017.05.002>
- Broz, P. (2015). Immunology: Caspase target drives pyroptosis. *Nature*, 526, 642–643. <https://doi.org/10.1038/nature15632>
- Brydges, S. D., Broderick, L., McGeough, M. D., Pena, C. A., Mueller, J. L., & Hoffman, H. M. (2013). Divergence of IL-1, IL-18, and cell death in NLRP3 inflammasomopathies. *Journal of Clinical Investigation*, 123, 4695–4705. <https://doi.org/10.1172/jci71543>
- Chen, G. Y., & Nunez, G. (2010). Sterile inflammation: Sensing and reacting to damage. *Nature Reviews Immunology*, 10, 826–837. <https://doi.org/10.1038/nri2873>
- Chen, Q., Jin, Y., Zhang, K., Li, H., Chen, W., Meng, G., & Fang, X. (2014). Alarmin HNP-1 promotes pyroptosis and IL-1 $\beta$  release through different roles of NLRP3 inflammasome via P2X7 in LPS-primed macrophages. *Innate Immunity*, 20, 290–300. <https://doi.org/10.1177/1753425913490575>
- Chen, X., He, W. T., Hu, L., Li, J., Fang, Y., Wang, X., ... Han, J. (2016). Pyroptosis is driven by non-selective gasdermin-D pore and its morphology is different from MLKL channel-mediated necroptosis. *Cell Research*, 26, 1007–1020. <https://doi.org/10.1038/cr.2016.100>
- Choi, Y. S., Kim, Y. C., Ji, S., & Choi, Y. (2014). Increased bacterial invasion and differential expression of tight-junction proteins, growth factors, and growth factor receptors in periodontal lesions. *Journal of Periodontology*, 85, e313–e322. <https://doi.org/10.1902/jop.2014.130740>
- Darveau, R. P., Pham, T. T., Lemley, K., Reife, R. A., Bainbridge, B. W., Coats, S. R., ... Hajjar, A. M. (2004). Porphyromonas gingivalis lipopolysaccharide contains multiple lipid A species that functionally interact with both toll-like receptors 2 and 4. *Infection and Immunity*, 72, 5041–5051. <https://doi.org/10.1128/iai.72.9.5041-5051.2004>
- de Vasconcelos, N. M., Van Opendenbosch, N., Van Gorp, H., Parthoens, E., & Lamkanfi, M. (2018). Single-cell analysis of pyroptosis dynamics reveals conserved GSDMD-mediated subcellular events that precede plasma membrane rupture. *Cell Death and Differentiation*, <https://doi.org/10.1038/s41418-018-0106-7>
- Ebe, N., Hara-Yokoyama, M., Iwasaki, K., Iseki, S., Okuhara, S., Podyma-Inoue, K. A., ... Izumi, Y. (2011). Pocket epithelium in the pathological setting for HMGB1 release. *Journal of Dental Research*, 90, 235–240. <https://doi.org/10.1177/0022034510385688>



- Evans, M., Murofushi, T., Tsuda, H., Mikami, Y., Zhao, N., Ochiai, K., ... Suzuki, N. (2016). Combined effects of starvation and butyrate on autophagy-dependent gingival epithelial cell death. *Journal of Periodontal Research*, 52(3), 522–531. <https://doi.org/10.1111/jre.12418>
- Fernandes-Alnemri, T., Wu, J., Yu, J. W., Datta, P., Miller, B., Jankowski, W., ... Alnemri, E. S. (2007). The pyroptosome: A supramolecular assembly of ASC dimers mediating inflammatory cell death via caspase-1 activation. *Cell Death and Differentiation*, 14, 1590–1604. <https://doi.org/10.1038/sj.cdd.4402194>
- Fink, S. L., & Cookson, B. T. (2006). Caspase-1-dependent pore formation during pyroptosis leads to osmotic lysis of infected host macrophages. *Cellular Microbiology*, 8, 1812–1825. <https://doi.org/10.1111/j.1462-5822.2006.00751.x>
- Galluzzi, L., & Kroemer, G. (2017). Secondary necrosis: Accidental no more. *Trends Cancer*, 3, 1–2. <https://doi.org/10.1016/j.trecan.2016.12.001>
- Groeger, S. E., & Meyle, J. (2015). Epithelial barrier and oral bacterial infection. *Periodontology 2000*, 69, 46–67. <https://doi.org/10.1111/prd.12094>
- Hammad, H., & Lambrecht, B. N. (2015). Barrier epithelial cells and the control of type 2 immunity. *Immunity*, 43, 29–40. <https://doi.org/10.1016/j.immuni.2015.07.007>
- He, W. T., Wan, H., Hu, L., Chen, P., Wang, X., Huang, Z., ... Han, J. (2015). Gasdermin D is an executor of pyroptosis and required for interleukin-1 $\beta$  secretion. *Cell Research*, 25, 1285–1298. <https://doi.org/10.1038/cr.2015.139>
- Herrmann, J. M., & Meyle, J. (2015). Neutrophil activation and periodontal tissue injury. *Periodontology 2000*, 69, 111–127. <https://doi.org/10.1111/prd.12088>
- How, K. Y., Song, K. P., & Chan, K. G. (2016). Porphyromonas gingivalis: An overview of periodontopathic pathogen below the gum line. *Frontiers in Microbiology*, 7, 1–14. <https://doi.org/10.3389/fmicb.2016.00053>
- Jiang, Z. L., Cui, Y. Q., Gao, R., Li, Y., Fu, Z. C., Zhang, B., & Guan, C. C. (2013). Study of TNF- $\alpha$ , IL-1 $\beta$  and LPS levels in the gingival crevicular fluid of a rat model of diabetes mellitus and periodontitis. *Disease Markers*, 34, 295–304. <https://doi.org/10.3233/dma-130974>
- Jin, L. (2011). An update on innate defense molecules of human gingiva. *Periodontology 2000*, 56, 125–142. <https://doi.org/10.1111/j.1600-0757.2010.00364.x>
- Jin, L. J., Lamster, I. B., Greenspan, J. S., Pitts, N. B., Scully, C., & Warnakulasuriya, S. (2016). Global burden of oral diseases: Emerging concepts, management and interplay with systemic health. *Oral Diseases*, 22, 609–619. <https://doi.org/10.1111/odi.12428>
- Kayagaki, N., Stowe, I. B., Lee, B. L., O'Rourke, K., Anderson, K., Warming, S., ... Dixit, V. M. (2015). Caspase-11 cleaves gasdermin D for non-canonical inflammasome signalling. *Nature*, 526, 666–671. <https://doi.org/10.1038/nature15541>
- Kayagaki, N., Wong, M. T., Stowe, I. B., Ramani, S. R., Gonzalez, L. C., Akashi-Takamura, S., ... Dixit, V. M. (2013). Noncanonical inflammasome activation by intracellular LPS independent of TLR4. *Science*, 341, 1246–1249. <https://doi.org/10.1126/science.1240248>
- Kerr, J. F., Gobe, G. C., Winterford, C. M., & Harmon, B. V. (1995). Anatomical methods in cell death. *Methods in Cell Biology*, 46, 1–27.
- Kusumoto, Y., Hirano, H., Saitoh, K., Yamada, S., Takedachi, M., Nozaki, T., ... Murakami, S. (2004). Human gingival epithelial cells produce chemotactic factors interleukin-8 and monocyte chemoattractant protein-1 after stimulation with Porphyromonas gingivalis via toll-like receptor 2. *Journal of Periodontology*, 75, 370–379. <https://doi.org/10.1902/jop.2004.75.3.370>
- LaRock, C. N., & Cookson, B. T. (2013). Burning down the house: Cellular actions during pyroptosis. *PLoS Path*, 9, 1–3. <https://doi.org/10.1371/journal.ppat.1003793>
- Li, Q., Meng, H., & Gao, X. (2012). Longitudinal study of volatile fatty acids in the gingival crevicular fluid of patients with periodontitis before and after nonsurgical therapy. *Journal of Periodontal Research*, 47, 740–749. <https://doi.org/10.1111/j.1600-0765.2012.01489.x>
- Lian, D., Dai, L., Xie, Z., Zhou, X., Liu, X., Zhang, Y., ... Chen, Y. (2018). Periodontal ligament fibroblasts migration injury via ROS/TXNIP/Nlrp3 inflammasome pathway with Porphyromonas gingivalis lipopolysaccharide. *Molecular Immunology*, 103, 209–219. <https://doi.org/10.1016/j.molimm.2018.10.001>
- Liu, X., & Lieberman, J. (2017). A Mechanistic understanding of pyroptosis: The fiery death triggered by invasive infection. *Advances in Immunology*, 135, 81–117. <https://doi.org/10.1016/bs.ai.2017.02.002>
- Liu, X., Zhang, Z., Ruan, J., Pan, Y., Magupalli, V. G., Wu, H., & Lieberman, J. (2016). Inflammasome-activated gasdermin D causes pyroptosis by forming membrane pores. *Nature*, 535, 153–158. <https://doi.org/10.1038/nature18629>
- Lu, B., Wang, H., Andersson, U., & Tracey, K. J. (2013). Regulation of HMGB1 release by inflammasomes. *Protein Cell*, 4, 163–167. <https://doi.org/10.1007/s13238-012-2118-2>
- Lu, R., Meng, H., Gao, X., Xu, L., & Feng, X. (2014). Effect of non-surgical periodontal treatment on short chain fatty acid levels in gingival crevicular fluid of patients with generalized aggressive periodontitis. *Journal of Periodontal Research*, 49, 574–583. <https://doi.org/10.1111/jre.12137>
- Meyle, J., & Chapple, I. (2015). (2015) Molecular aspects of the pathogenesis of periodontitis. *Periodontology 2000*, 69, 7–17. <https://doi.org/10.1111/prd.12104>
- Nakagawa, T., Shimizu, S., Watanabe, T., Yamaguchi, O., Otsu, K., Yamagata, H., ... Tsujimoto, Y. (2005). Cyclophilin D-dependent mitochondrial permeability transition regulates some necrotic but not apoptotic cell death. *Nature*, 434, 652–658. <https://doi.org/10.1038/nature03317>
- Nethravathy, R. R., Alamelu, S., Arun, K. V., & Kumar, T. S. (2014). Evaluation of circulatory and salivary levels of heat shock protein 60 in periodontal health and disease. *Indian Journal of Dental Research*, 25, 300–304. <https://doi.org/10.4103/0970-9290.138317>
- Niederman, R., Buyle-Bodin, Y., Lu, B. Y., Robinson, P., & Naleway, C. (1997a). Short-chain carboxylic acid concentration in human gingival crevicular fluid. *Journal of Dental Research*, 76, 575–579. <https://doi.org/10.1177/00220345970760010801>
- Niederman, R., Zhang, J., & Kashket, S. (1997b). Short-chain carboxylic-acid-stimulated, PMN-mediated gingival inflammation. *Critical Reviews in Oral Biology and Medicine*, 8, 269–290. <https://doi.org/10.1177/10454411970080030301>
- Oda, D., & Watson, E. (1990). Human oral epithelial cell culture I. Improved conditions for reproducible culture in serum-free medium. *In Vitro Cellular & Developmental Biology*, 26, 589–595. <https://doi.org/10.1007/BF02624208>
- Rogers, C., Fernandes-Alnemri, T., Mayes, L., Alnemri, D., Cingolani, G., & Alnemri, E. S. (2017). Cleavage of DFNA5 by caspase-3 during apoptosis mediates progression to secondary necrotic/pyroptotic cell death. *Nature Communications*, 8, 1–14. <https://doi.org/10.1038/ncomms14128>
- Russo, H. M., Rathkey, J., Boyd-Tressler, A., Katsnelson, M. A., Abbott, D. W., & Dubyak, G. R. (2016). Active caspase-1 induces plasma membrane pores that precede pyroptotic lysis and are blocked by lanthanides. *The Journal of Immunology*, 197, 1353–1367. <https://doi.org/10.4049/jimmunol.1600699>
- Singer, R. E., & Buckner, B. A. (1981). Butyrate and propionate: Important components of toxic dental plaque extracts. *Infection and Immunity*, 32, 458–463.
- Smith, M., Seymour, G. J., & Cullinan, M. P. (2010). Histopathological features of chronic and aggressive periodontitis. *Periodontology 2000*, 53, 45–54. <https://doi.org/10.1111/j.1600-0757.2010.00354.x>
- Sun, G. W., Lu, J., Pervaiz, S., Cao, W. P., & Gan, Y. H. (2005). Caspase-1 dependent macrophage death induced by Burkholderia pseudomallei. *Cellular Microbiology*, 7, 1447–1458. <https://doi.org/10.1111/j.1462-5822.2005.00569.x>

- Sun, X., Meng, H., Shi, D., Xu, L., Zhang, L., Chen, Z., ... Lu, R. (2011). Analysis of plasma calprotectin and polymorphisms of S100A8 in patients with aggressive periodontitis. *Journal of Periodontal Research*, 46, 354–360. <https://doi.org/10.1111/j.1600-0765.2011.01350.x>
- Thunell, D. H., Tymkiw, K. D., Johnson, G. K., Joly, S., Burnell, K. K., Cavanaugh, J. E., ... Guthmiller, J. M. (2010). A multiplex immunoassay demonstrates reductions in gingival crevicular fluid cytokines following initial periodontal therapy. *Journal of Periodontal Research*, 45, 148–152. <https://doi.org/10.1111/j.1600-0765.2009.01204.x>
- Tonetti, M., Eftimiadi, C., Damiani, G., Buffa, P., Buffa, D., & Botta, G. A. (1987). Short chain fatty acids present in periodontal pockets may play a role in human periodontal diseases. *Journal of Periodontal Research*, 22, 190–191. <https://doi.org/10.1111/j.1600-0765.1987.tb01565.x>
- Tonetti, M. S., Jepsen, S., Jin, L., & Otomo-Corgel, J. (2017). Impact of the global burden of periodontal diseases on health, nutrition and wellbeing of mankind: A call for global action. *Journal of Clinical Periodontology*, 44, 456–462. <https://doi.org/10.1111/jcpe.12732>
- Tsuda, H., Ochiai, K., Suzuki, N., & Otsuka, K. (2010). Butyrate, a bacterial metabolite, induces apoptosis and autophagic cell death in gingival epithelial cells. *Journal of Periodontal Research*, 45, 626–634. <https://doi.org/10.1111/j.1600-0765.2010.01277.x>
- Tsybikov, N. N., Baranov, S. V., Kuznik, B. I., Malezhik, L. P., & Isakova, N. V. (2014). Serum, oral and gingival fluid levels of heat shock protein-70, cytokines and their autoantibodies by periodontal disease. *Stomatologija (Mosk)*, 93, 16–18.
- Vande Walle, L., & Lamkanfi, M. (2016). Pyroptosis. *Current Biology*, 26, R568–572. <https://doi.org/10.1016/j.cub.2016.02.019>
- Wang, Y., Gao, W., Shi, X., Ding, J., Liu, W., He, H., ... Shao, F. (2017). Chemotherapy drugs induce pyroptosis through caspase-3 cleavage of a Gasdermin. *Nature*, 547(7661), 99–103. <https://doi.org/10.1038/nature22393>
- Xie, P., Deng, L. X., Gong, P., Ding, Y., & Tang, X. H. (2011). Expression of HMGB1 and HMGN2 in gingival tissues, GCF and PICF of periodontitis patients and peri-implantitis. *Brazilian Journal of Microbiology*, 42, 1213–1219. <https://doi.org/10.1590/s1517-838220110003000047>
- Yu, X., Shahir, A. M., Sha, J., Feng, Z., Eapen, B., Nithianantham, S., ... Ye, F. (2014). Short-chain fatty acids from periodontal pathogens suppress histone deacetylases, EZH2, and SUV39H1 to promote Kaposi's sarcoma-associated herpesvirus replication. *Journal of Virology*, 88, 4466–4479. <https://doi.org/10.1128/jvi.03326-13>
- Zhang, C. C., Li, C. G., Wang, Y. F., Xu, L. H., He, X. H., Zeng, Q. Z., ... Ouyang, D. Y. (2019). Chemotherapeutic paclitaxel and cisplatin differentially induce pyroptosis in A549 lung cancer cells via caspase-3/GSDME activation. *Apoptosis*, 24(3-4), 312–325. <https://doi.org/10.1007/s10495-019-01515-1>
- Zhang, J., Li, L., Peng, Y., Chen, Y., Lv, X., Li, S., ... Liu, Y. (2018). Surface chemistry induces mitochondria-mediated apoptosis of breast cancer cells via PTEN/PI3K/AKT signaling pathway. *Biochimica Et Biophysica Acta (BBA) - Molecular Cell Research*, 1865, 172–185. <https://doi.org/10.1016/j.bbamcr.2017.10.007>
- Zhou, R., Yazdi, A. S., Menu, P., & Tschopp, J. (2011). A role for mitochondria in NLRP3 inflammasome activation. *Nature*, 469, 221–225. <https://doi.org/10.1038/nature09663>

## SUPPORTING INFORMATION

Additional supporting information may be found online in the Supporting Information section at the end of the article.

**How to cite this article:** Liu J, Wang Y, Meng H, et al. Butyrate rather than LPS subverts gingival epithelial homeostasis by downregulation of intercellular junctions and triggering pyroptosis. *J Clin Periodontol*. 2019;46:894–907. <https://doi.org/10.1111/jcpe.13162>